Research Article | Vol. 25, No. 8 | 17 Apr 2017 | OPTICS EXPRESS 8484

Optics EXPRESS

Terahertz optical bistability of graphene in thin layers of dielectrics

KWANG JUN AHN[1,4] AND FABIAN ROTERMUND[2,3]

[1]*Department of Energy Systems Research and Department of Physics, Ajou University, Suwon 16499, South Korea*
[2]*Department of Physics, Korea Advanced Institute of Science and Technology (KAIST), Daejeon 34141, South Korea*
[3]*rotermund@kaist.ac.kr*
[4]*kjahn@ajou.ac.kr*

Abstract: We theoretically studied in terahertz frequency regime optical bistability of graphene placed at the interface between thin dielectric layers. We solved self-consistently the nonlinear wave equations containing the third-order optical conductivity of graphene in four-layer structures and obtained hysteresis response of the transmitted power as a function of the incident power. We numerically observed that the critical powers for the up and down transitions and the Fermi-energy of graphene required for terahertz optical bistability can be reduced by carefully choosing material properties and the thicknesses of dielectric layers. Furthermore, these values can be substantially decreased when graphene as a randomly stacked multilayer structure is asymmetrically located in thin dielectric layers.

OCIS codes: (190.1450) Bistability; (190.3270) Kerr effect; (310.6860) Thin films, optical properties; (230.4320) Nonlinear optical devices.

References and links

1. S. D. Smith,"Lasers, nonlinear optics and optical computers," Nature **316**, 319–324 (1985).
2. E. Abraham and S. D. Smith, "Optical bistability and related devices," Rep. Prog. Phys. **45**, 815–885 (1982).
3. Robert W. Boyd, *Nonlinear Optics* (Elsevier Inc., 2008).
4. Michael P. Marder, *Condensed Matter Physics* (John Wiley & Sons, Inc., 2010).
5. M. Seo, J. Kyoung, H. Park, S. Koo, H.-s. Kim, H. Bernien, B. J. Kim, J. H. Choe, Y. H. Ahn, H.-T. Kim, N. Park, Q. H. Park, K. Ahn, and D.-s. Kim, "Active terahertz nanoantennas based on VO_2 phase transition," Nano Lett. **10**, 2064–2068 (2010).
6. G. A. Wurtz, R. Pollard, and A. V. Zayats, "Optical bistability in nonlinear surface-plasmon polaritonic crystals," Phys. Rev. Lett. **97**, 057402 (2006).
7. Sergio G. Rodrigo, S. Carretero-Palacios, F. J. García-Vidal, and L. Martín-Moreno, "Metallic slit arrays filled with third-order nonlinear media: Optical Kerr effect and third-harmonic generation," Phys. Rev. B **83**, 235425 (2011).
8. S. Schmitt-Rink, D. A. B. Miller and D. S. Chemla, "Theory of the linear and nonlinear optical properties of semiconductor microcrystallites," Phys. Rev. B **35**, 8113–8125 (1987).
9. Sukang Bae, Hyeongkeun Kim, Youngbin Lee, Xiangfan Xu, Jae-Sung Park, Yi Zheng, Jayakumar Balakrishnan, Tian Lei, Hye Ri Kim, Young Il Song, Young-Jin Kim, Kwang S. Kim, Barbaros Özyilmaz, Jong-Hyun Ahn, Byung Hee Hong and Sumio Iijima, "Roll-to-roll production of 30-inch graphene films for transparent electrodes," Nature Nanotech. **5**, 574–578 (2010).
10. K. S. Novoselov, V. I. Fal'ko, L. Colombo, P. R. Gellert, M. G. Schwab and K. Kim, "A roadmap for graphene," Nature **490**, 192–200 (2012).
11. Thomas Christensen, Wei Yan, Antti-Pekka Jauho, Martijn Wubs, and N Asger Mortensen, "Kerr nonlinearity and plasmonic bistability in graphene nanoribbons," Phys. Rev. B **92**, 121407(R) (2015).
12. J. L. Cheng, N. Vermeulen, and J. E. Sipe, "Third-order nonlinearity of graphene: Effects of phenomenological relaxation and finite temperature," Phys. Rev. B **91**, 235320 (2015).
13. S. A. Mikhailov, "Quantum theory of the third-order nonlinear electrodynamic effects of graphene," Phys. Rev. B **93**, 085403 (2016).
14. T. Gu, N. Petrone, J. F. McMillan, A. van der Zande, M. Yu, G. Q. Lo, D. L. Kwong, J. Hone and C. W. Wong, "Regenerative oscillation and four-wave mixing in graphene optoelectronics," Nature Photon. **6**, 554–559 (2012).
15. Qiaoliang Bao, Jianqiang Chen, Yuanjiang Xiang, Kai Zhang, Shaojuan Li, Xiaofang Jiang, Qing-Hua Xu, Kian Ping Loh, and T. Venkatesan, " Graphene Nanobubbles: A new optical nonlinear material," Adv. Optical Mater. **3**, 744–749 (2015).

#286657 https://doi.org/10.1364/OE.25.008484
Journal © 2017 Received 14 Feb 2017; revised 23 Mar 2017; accepted 24 Mar 2017; published 3 Apr 2017

Optics EXPRESS

16. Yuanjiang Xiang, Xiaoyu Dai, Jun Guo, Shuangchun Wen, and Dingyuan Tang, "Tunable optical bistability at the graphene-covered nonlinear interface,", Appl. Phys. Lett. **104**, 051108 (2014).
17. Xiaoyu Dai, Leyong Jiang and Yuanjiang Xiang, "Low threshold optical bistability at terahertz frequencies with graphene surface plasmons," Sci. Rep. **5**, 12271 (2015).
18. Xiaoyu Dai, Leyong Jiang, and Yuanjiang Xiang, " Tunable optical bistability of dielectric/nonlinear graphene/dielectric heterostructures,", Opt. Express **23**, 6497–6508 (2015).
19. In Hyung Baek, Joachim Hamm, Kwang Jun Ahn, Bong Joo Kang, Sang Soon Oh, Sukang Bae, Sun Young Choi, Byung Hong, Dong-Il Yeom, Bumki Min, Ortwin Hess, Young Uk Jeong, and Fabian Rotermund, "Boosting the terahertz nonlinearity of graphene by orientation disorder," 2D Mater. **4**, 025035 (2017).
20. E. Lidorikis, K. Busch, Qiming Li, C. T. Chan, C. M. Soukoulis, "Optical nonlinear response of a single nonlinear dielectric layer sandwiched between two linear dielectric structures," Phys. Rev. B **56**, 15090 (1997).
21. I. H. Baek, K. J. Ahn, B. J. Kang, S. Bae, B. H. Hong, D.-I. Yeom, K. Lee, Y. U. Jeong, and F. Rotermund, "Terahertz transmission and sheet conductivity of randomly stacked multi-layer graphene," Appl. Phys. Lett. **102**, 191109 (2013).
22. N. M. R. Peres, Yu. V. Bludov, Jaime E. Santos, Antti-Pekka Jauho, and M. I. Vasilevskiy, "Optical bistability of graphene in the terahertz range," Phys. Rev. B **90**, 125425 (2014).
23. Jason Horng, Chi-Fan Chen, Baisong Geng, Caglar Girit, Yuanbo Zhang, Zhao Hao, Hans A. Bechtel, Michael Martin, Alex Zettl, Michael F. Crommie, Y. Ron Shen, and Feng Wang, " Drude conductivity of Dirac fermions in graphene," Phys. Rev. B **83**, 165113 (2011).
24. R. Bonifacio and L. A. Lugiato, "Optical bistability and cooperative effects in resonance fluorescence," Phys. Rev. A **18**, 1129–1144 (1978).

1. Introduction

Optical bistability (OB) is the fundamental operation of components constructing optical computers such as optical memory, switch, and amplifier [1]. OB is typically characterized by a hysteresis response to the input field [2, 3]. For a same input value, nonlinear optical systems can have different responses depending on roots of the systems. For instances, a system governed by third-order nonlinearities can have three solutions while it has only one in linear optical regime. OB accompanied by memory effect can be observed mostly in strongly correlated electronic systems [4] and phase transition materials [5]. Anyways, the memory effect shown by such material is originated from different physical backgrounds. In general, OB is induced by abrupt changes of transmitted/reflected light caused by nonlinear refractive index or absorption coefficient of materials and strong electric field intensities in cavities as feedback [6, 7], although OB without feedback is also suggested [8].

Since single layer of carbon atoms has successfully been isolated from bulk graphite and can now be chemically synthesized on wafer scales [9], the unique electric and optical properties of graphene have been intensively studied for the next generation of electric transport and optical materials [10]. In special, many theoretical [11–13] and experimental studies [14, 15] demonstrate that graphene should have strong third-order nonlinearities in terahertz (THz) frequency regime, which motivate to suggest diverse geometries and physical mechanisms incorporated with graphene to produce energy efficient OB in ultra subwavelength scales. Examples are graphene between a half-infinite linear dielectric and a Kerr medium [16], and graphene sandwiched by two finite dielectrics [17, 18].

In this report, we theoretically investigate THz OB of graphene embedded in thin dielectric layers. By solving boundary conditions and determining the electric field at the graphene position self-consistently, we can derive an analytical solution for THz OB of graphene. In special, we present a critical condition for the occurrence of THz OB with graphene at the interface between two dielectrics. While previous studies have mainly focused on graphene plasmon resonance [17] or OB near the angles corresponding to total internal reflection [18], our consideration is fixed to the normal incidence, which is more favorable situation for experiment. In addition, we show that the threshold power for THz OB can be reduced by one order of magnitude, if highly doped monolayer graphene is replaced by randomly stacked multilayer graphene, where the nonlinear optical properties of monolayer graphene can be well preserved [19].

Optics EXPRESS

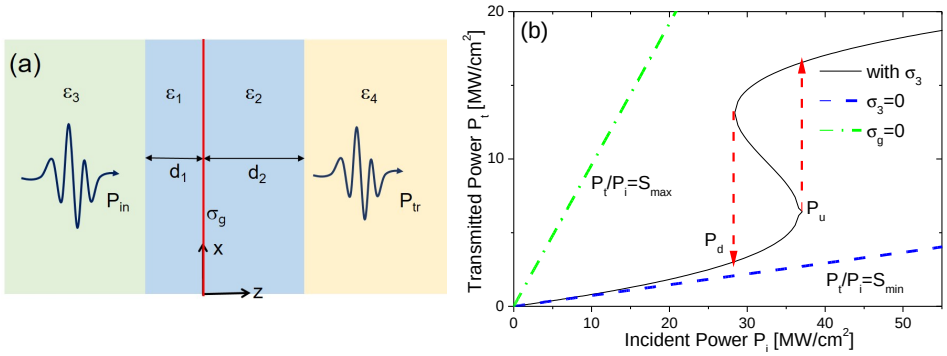

Fig. 1. (a) The sample geometry considered in this study. Graphene with optical conductivity σ_g is sandwiched by two finite dielectric layers ϵ_1 and ϵ_2 with thicknesses d_1 and d_2. (b) THz OB of graphene at the interface between $\epsilon_1 = \epsilon_3 = 2.25$ and $\epsilon_2 = \epsilon_4 = 1$ ($E_F = 1.2\,eV$, $\omega = 2\pi$ THz). The hysteresis curve is bounded by two lines, $P_t/P_i = S_{\max}$ for $\sigma_g = 0$ and $P_t/P_i = S_{\min}$ for $\sigma_3 = 0$. The critical powers for the up- and down-transition are read as $P_u = 36.7\,MW/cm^2$ and $P_d = 27.8\,MW/cm^2$, respectively.

2. Mathematical model

The configuration of the system considered in this study is presented in Fig. 1(a) where graphene with an optical conductivity σ_g is located at the interface between two thin dielectric layers ϵ_1 and ϵ_2 [20]. The thicknesses of both layers are d_1 and d_2 along the z-axis. The electric fields in four divided regions are expressed as

$$E_x(z) = \begin{cases} E_0 e^{ik_{3z}(z+d_1)} + re^{-ik_{3z}(z+d_1)} & (z < -d_1) \\ A_1 e^{ik_{1z}z} + B_1 e^{-ik_{1z}z} & (-d_1 < z < 0) \\ A_2 e^{ik_{2z}(z-d_2)} + B_2 e^{-ik_{2z}(z-d_2)} & (0 < z < d_2) \\ te^{ik_{4z}(z-d_2)} & (z > d_2), \end{cases} \tag{1}$$

where $k_{jz} = 2\pi\sqrt{\epsilon_j}/\lambda$ are the wave numbers in each region ($j = 1, \cdots, 4$). With the optical conductivity $\sigma_g = \sigma_1 + \sigma_3|E_x(0)|^2$, the amplitude coefficients A_1, A_2, B_1, B_2, and r are determined by the Dirichlet and Neumann boundary conditions, a similar procedure presented in [21]. It should be noted that due to the nonlinear optical conductivity coupled to the electric field $\sigma_3|E_x(0)|^2$, the amplitude coefficients must be self-consistently determined. Since we are mainly interested in OB of graphene at around 1 THz, the linear (first order) optical conductivity σ_1 is mainly determined by the intraband contribution

$$\sigma_1(\omega) = \sigma_{1r} + i\sigma_{1i} = \frac{2e_0^2 k_B T}{\pi\hbar^2} \frac{i}{\omega + i\Gamma} \log\left[2\cosh\left(\frac{E_F}{2k_B T}\right)\right] \tag{2}$$

and the nonlinear conductivity is expressed by the third order optical conductivity σ_3 derived from the Boltzmann's transport equation within the relaxation time approximation [22]

$$\sigma_3(\omega) = -\frac{3}{4}\frac{e_0^2(e_0 v_F)^2}{\pi\hbar^2 E_F}\left\{\frac{2}{(\Gamma^2+\omega^2)(\Gamma - i\omega)} + \frac{1}{(\Gamma - i\omega)^2(\Gamma - 2i\omega)}\right\} \tag{3}$$

$$\approx \sigma_{3i} = -i\frac{9}{8}\frac{e_0^2(e_0 v_F)^2}{\pi\hbar^2 E_F \omega^3} \quad \text{for } \omega \gg \Gamma \tag{4}$$

where e_0 is the elementary charge, k_B the Boltzmann constant, T temperature, $\hbar$ the Planck constant over 2π, Γ the decay rate of plasma, and E_F (v_F) the Fermi-energy (velocity). Finally,

Optics EXPRESS

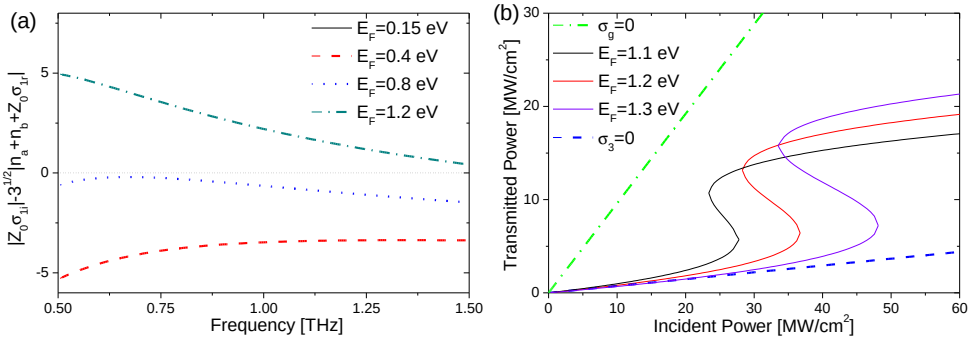

Fig. 2. (a) The second criterion for THz OB of graphene in single interface system ($n_a = 1,\ n_b = 1.5$) as a function of frequency for different values of Fermi-energy. (b) THz OB of graphene for different values of E_F for the same conditions as (a).

the incident field amplitude E_0 has a cubic dependence on the transmission coefficient t as

$$E_0 = \left[\frac{n_2}{2n_1}(a_1 - b_1)(a_2 - b_2) + \frac{1}{2}(a_1 + b_1)(a_2 + b_2) + \frac{Z_0\sigma_1}{2n_1}(a_1 - b_1)(a_2 + b_2)\right] t$$
$$- \frac{Z_0\sigma_3}{2n_1}(a_1 - b_1)(a_2 + b_2)^3 t^3 = \alpha t - \beta t^3 \tag{5}$$

where Z_0 denotes the free space impedance, $n_j = \sqrt{\epsilon_j}$ are the refractive indices, and $a_{1/2}$ and $b_{1/2}$ are defined as

$$a_1 = \frac{1}{2}(1 + \frac{k_{1z}}{k_{3z}})e^{-ik_{1z}d_1}, \quad b_1 = \frac{1}{2}(1 - \frac{k_{1z}}{k_{3z}})e^{ik_{1z}d_1}, \tag{6}$$

$$a_2 = \frac{1}{2}(1 + \frac{k_{4z}}{k_{2z}})e^{-ik_{2z}d_2}, \quad b_2 = \frac{1}{2}(1 - \frac{k_{4z}}{k_{2z}})e^{ik_{2z}d_2}. \tag{7}$$

By performing the absolute square on the both sides of Eq. (5), one obtains an ordinary cubic equation

$$Y = |E_0|^2 = |\alpha|^2 t^2 - (\alpha\beta^* + \alpha^*\beta)t^4 + |\beta|^2 t^6$$
$$= AX - CX^2 + BX^3 \tag{8}$$

where by new definitions $Y = |E_0|^2$ and $X = t^2$ a complex-valued incident field but the real-valued transmitted field amplitude are implicitly assumed.

3. Analytical approach and numerical results

It is well known that cubic equations such as Eq. (8) have three different solutions only when two extrema exist:

$$\frac{dY}{dX} = 3BX^2 - 2CX + A = 0 \ \Leftrightarrow\ X_{d/u} = \frac{1}{3B}(C \pm \sqrt{C^2 - 3AB}). \tag{9}$$

Because both X_d and X_u must have positive real values [cp. Fig. 1(b)], it is additionally required that

$$C > \sqrt{C^2 - 3AB} \quad \text{and} \quad C^2 > 3AB. \tag{10}$$

Optics EXPRESS

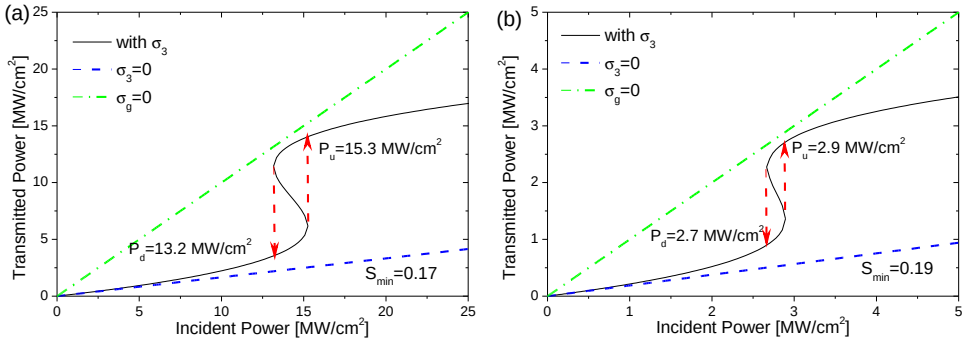

Fig. 3. (a) THz OB of graphene in an asymmetric four-layered system. The physical parameters used are $\epsilon_1 = \epsilon_2 = 1.55^2$, $\epsilon_3 = \epsilon_4 = 1.5^2$, $d_1 = 200\,nm$, $d_2 = 2200\,nm$, and $E_F = 0.9\,eV$. (b) THz OB of a bilayer graphene in an asymmetric four-layered system. The physical parameters used are $\epsilon_1 = \epsilon_2 = 1.55^2$, $\epsilon_3 = \epsilon_4 = 1.5^2$, $d_1 = 600\,nm$, $d_2 = 4800\,nm$, and $E_F = 0.4\,eV$.

While the former condition is always true ($AB = |\alpha|^2|\beta|^2 > 0$), the latter must be discussed in explicit situations.

We consider THz OB of graphene in single interface system to make it as simple as possible. By substituting $n_b^2 = \epsilon_1 = \epsilon_3$, $n_a^2 = \epsilon_2 = \epsilon_4$ and $d_1 = d_2 = 0$, Eq. (5) is simplified to

$$E_0 = \left[\frac{1}{2}\left(\frac{n_a}{n_b} + 1\right) + \frac{Z_0\sigma_{1r}}{2n_b} + i\frac{Z_0\sigma_{1i}}{2n_b}\left(1 - \frac{\sigma_{3i}}{\sigma_{1i}}t^2\right)\right]t. \tag{11}$$

Then, the second criterion of Eq. (10) requires

$$|Z_0\sigma_{1i}| > \sqrt{3}\,|(n_a + n_b) + Z_0\sigma_{1r}|\,. \tag{12}$$

Furthermore, the OB of graphene embedded in a multilayer structure must be restricted within the area bordered by two lines, as displayed in Fig. 1(b). The upper limit ($X/Y \propto S_{\max}$) corresponding to the maximum transparency is the case without graphene ($\sigma_g = 0$), and the lower one ($X/Y \propto S_{\min}$) for the maximum opacity is given when the third-order conductivity of graphene is zero ($\sigma_3 = 0$), due to its negative imaginary value.

In Fig. 2(a) we plot the second condition, Eq. (12) for different values of the Fermi-energy where $T = 300\,K$ and the decay rate of plasma is decided by mobility of graphene $\mu_g = 10^4\,cm^2/Vs$ and the Fermi-energy ($\Gamma = e_0 v_F^2/(\mu_g E_F)$) [23]. Together with Fig. 2(b), it is clearly seen that the THz OB of graphene in the single interface system can be generated when $E_F > 1.0\,eV$. However, because the solutions of the cubic equation between two critical values X_d and X_u are known to be physically unstable [24], the system's response to the increasing (decreasing) input is abruptly changed to another branch as depicted by red dashed arrows in Fig. 1(b). Due to the sufficiently small real part of the linear conductivity compared to the imaginary one for higher Fermi-energies($E_F > 1\,eV$), two critical values X_d and X_u are determined as

$$X_{d/u} = \frac{1}{3}\frac{\sigma_{1i}}{\sigma_{3i}}\left(1 \pm \sqrt{1 - \left(\frac{n_a + n_b}{Z_0\sigma_{1i}}\right)^2}\right). \tag{13}$$

For increasing Fermi-energy σ_{1i} increases, but σ_{3i} decreases as found in Eq. (4). Because $X_{d/u}$ and their counterparts of input $Y_{d/u} \propto P_{d/u}$ depend critically on the ratio σ_{1i}/σ_{3i}, larger

Optics EXPRESS

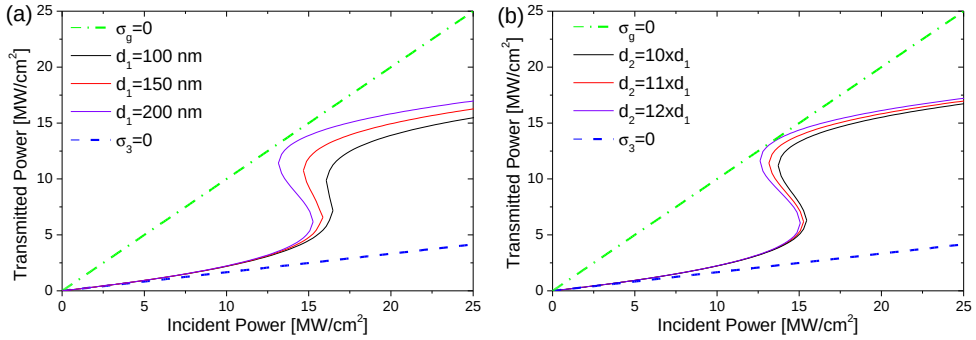

Fig. 4. (a) THz OB of graphene in an asymmetric four-layered system for different values of thickness d_1 with a fixed ratio $d_2/d_1 = 11$. Otherwise, the same physical parameters as Fig. 3(a) are used. (b) THz OB of graphene in an asymmetric four-layered system for different ratios d_2/d_1 with a fixed value of $d_1 = 200\,nm$. Otherwise, the same physical parameters as Fig. 3(a) are used.

modulation powers ($\Delta Y = Y_u - Y_d$) and modulation depths ($\Delta X = X_d - X_u$) are obtained for the increasing Fermi-energy, as demonstrated in Fig. 2(b).

Although THz OB can be produced by graphene in single interface system at the normal incidence, the required Fermi-energy and the critical input powers for the up (down)-transition are exceptionally very high. In order to reduce those values, graphene is supposed to be asymmetrically located in thin dielectric layers as shown in Fig. 3(a). Here, graphene is embedded in a relatively higher refractive index material ($n_1 = n_2 = 1.55$) covered by a lower one ($n_3 = n_4 = 1.5$). With a distance ratio of over ten ($d_2/d_1 = 11,\ d_1 = 200\,nm$) the critical power for the up- and down-transition are reduced by a factor of two. Especially, the Fermi-energy of graphene needed for THz OB is decreased to below $E_F < 1\,eV$, which is not sufficient for graphene in single interface systems [cp. Fig. 2(a) and 2(b)].

Further decrease of the critical powers and the Fermi-energy level for THz OB can be accomplished by using randomly stacked multilayer graphene. Recently, it has been shown that optical nonlinearities of graphene in THz frequency range can be preserved in randomly stacked multilayer graphene films [19]. By using the same combination of materials and changing both thicknesses to $d_1 = 600\,nm$ and $d_2 = 4800\,nm$, a complete hysteresis curve can be generated by one order of magnitude smaller incident powers, as represented in Fig. 3(b). Here, a bilayer graphene with Fermi-energy $E_F = 0.4\,eV$ is assumed. Additionally, the critical powers are reduced to several MW/cm^2. Such a tendency of lowered critical powers numerically observed in Fig. 1(b), and Fig. 3(a) and 3(b) results from narrowing the allowed power range for THz OB. As already discussed, OB arising in thin dielectric layers is bounded by two lines. While the upper limit determined by the transmission without graphene ($\sigma_g = 0$) is almost same for three cases, the lower boundary varies from $S_{\min} = 0.07$ in the single interface system of Fig. 1(b), $S_{\min} = 0.17$ for Fig. 3(a), and $S_{\min} = 0.19$ for Fig. 3(b).

Finally, the influence of thicknesses d_1 and d_2 on THz OB is investigated in Fig. 4. In Fig. 4(a) d_1 is changed from $d_1 = 100\,nm$ to $d_1 = 200\,nm$, while the thickness ratio is fixed to $d_2/d_1 = 11$. On the contrary, in Fig. 4(b) the thickness ratio is varied from $d_2/d_1 = 10$ to $d_2/d_1 = 12$ for a constant thickness of $d_1 = 200\,nm$. Note that the upper and lower limits do not change in both figures.

Optics EXPRESS

4. Conclusion

In summary, we theoretically studied THz OB of graphene embedded in thin dielectric layered systems. By self-consistently solving nonlinear wave equations including the third-order conductivity of graphene, we could derive hysteresis behavior of the transmitted power as a function of the incident power. We were able to derive a fully analytical solution for THz OB of graphene in single interface system. However, the critical powers and the Fermi-energy level are critically high. In order to decrease those values, graphene is suggested to be asymmetrically placed in four dielectric layers. Further lowering of the critical powers and the Fermi-energy were numerically demonstrated by using a randomly stacked bilayer graphene. Our studies can significantly contribute to constructing optical memory and switching devices based on graphene for optical computers.

Funding

National Research Foundation of Korea (NRF) Grants funded by the Korean Government (MSIP) (2014R1A2A1A11049467, 2016R1A2A1A05005381); Center for Advanced Meta-Materials (CAMM) funded by Korea Government (MSIP) as Global Frontier Project (2014M3A6B3063709).